Advances in Dynamical Systems and Applications.
ISSN 0973-5321, Volume 17, Number 2, (2022) pp. 497-522

https://www.ripublication.com/adsa.htm

Bond Graph Modelling of a Hybrid Solar Energy System For Medical Oxygen and Electricity Production in a Hospital

Jacques Francis Bakehe[1*], Simon Koumi Ngoh[1], Jean Gaston Tamba[1]
[1] *Technology and Applied Science Laboratory of the University of Douala*

Abstrat

The aim of this work is to propose the use of the bond graph (BG) language to model and simulate an off grid autonomous hybrid network consisting of a photovoltaic (PV) generator, an electrolyzer (EL), and a fuel cell used as green electricity and medical oxygen source for a hospital. The system is sized to suit the requirements of daily oxygen therapy needs of a hospital comprising a resuscitation room, a neonatal room, and a unit for the management of COVID-19 patients in respiratory distress. The system sized to meet a demand of 20 Nm^3/day of oxygen, requires a 40.45 kW PV array, a 19.34 kW electrolyzer, and a 15 kW fuel cell. The simulation of the system components was conducted under tropical climate using their bond graph model. During the sunniest day, the oxygen production would be 39.37 Nm^3/day oxygen while covering the electricity needs of the hospital building. For the least sunny day of the year, an oxygen production of 14.61 Nm^3/day was estimated. The proposed system could be an alternative option for onsite medical oxygen production.

Keywords: Solar energy, Water electrolysis, Oxygen, Hospital.

INTRODUCTION

Energy is a vital resource for every industrial society's development. Unfortunatly, the employment of this energy, which is mostly derived from fossil fuels, has significant societal implications including greenhouse gas emissions, floods, climate change. The world faces a responsibility to achieve an energy transition, which may be assured by a major integration of renewable energy sources into the energy mix. Unfortunately, due to a lack of full understanding of renewable energy systems and associated technologies, this integration remains problematic.

Modelling, simulation, and experimentation are being used throughout the world to better knowledge of renewable energy systems used alone or in combination with other technologies such as electrolyzers and fuel cells. Concerning PEM electrolyzers and related technologies, several models have been developed in the literature. These

models are available at several modeling sizes, ranging from the cell core to the entire PEMFC or PEMEL system. [1] introduced an equivalent electrical circuit (EEC) for electrical and thermal phenomena modeling in electrolyzer. [2] suggested a macroscopic energy representation (EMR) model of PEM electrolyzer. [3], have offered various EECs for the PEMFC's electrical model. Other authors, have either studied the real experimental system or used continuous models based on equations that only describe the steady state of each component [4-20].

The bond graph model have gained particular attention and are being used by numerous researchers for partial or total representation of energy production system including a PV generator, an electrolyzer, a fuel cells, and other auxiliary components during the last decade. Andouisi et al. in [21] employed a BG model to build an analytical average model of the PV-DC/DC system. In [22], Saida and Aissa established a mathematical model for PV modules based on the production data sheet, ambient temperature, and solar irradiation. This mathematical model of the solar module is converted to its single diode equivalent electrical circuit using bond graph methods. In their paper [23], Dhafer et al. recommend bond graph modeling to study a station of pump connected to a photovoltaic (PV) generator, while Mohamed Louzazni et al. present bond graph methods to dynamically model a PV generator in [24]. The dynamic model of the PEMFC is commonly provided utilizing the EEC, EMR, or BG [3] as a multidisciplinary device.

Chatti et al. [25] demonstrate the use of a single representation for not only the structural model but also the identification of problems that may damage the fuel cell using bond graph modeling. Abdallah et al. [26] offer a Bond Graph (BG) model of a system with multiple sources that includes a wind turbine and solar PV panels for hydrogen production by electrolysis of water. Badoud et al. [27] give a full bond graph modeling of a hybrid photovoltaic-fuel cell-electrolyzer-battery system. They use multi-physics models to account for temperature has an impact on electrochemical parameters in their research.

The purpose of this study is to develop a BG model of a hybrid energy system consisting of a PV array, an electrolyzer, and a fuel cell, dedicated to the production of green electricity and medical oxygen for a hospital. The simulation of the system designed and modeled is performed using 20sim software. First, the BG modelling of the system's different components will be carried out, and secondly, the system and its components will be simulated with under tropical atmospheric conditions characterized by a high solar radiation potential.

1. system sizing and modelling

1.1. System architecture and description

For this, we plan to use the solar energy source to produce both electricity and oxygen through an electrolyzer. The overview diagram of the system is shown in Figure 1.

- A solar generator as the main source of energy;

- A load simulating the end-user's consumption as the main load;
- A DC bus;
- Converters for adjusting voltages to the DC bus voltage;
- An electrolyzer that converts electrical energy into chemical energy;
- A fuel cell that converts chemical energy into electrical energy;
- A storage tank for the gases produced (oxygen and hydrogen).

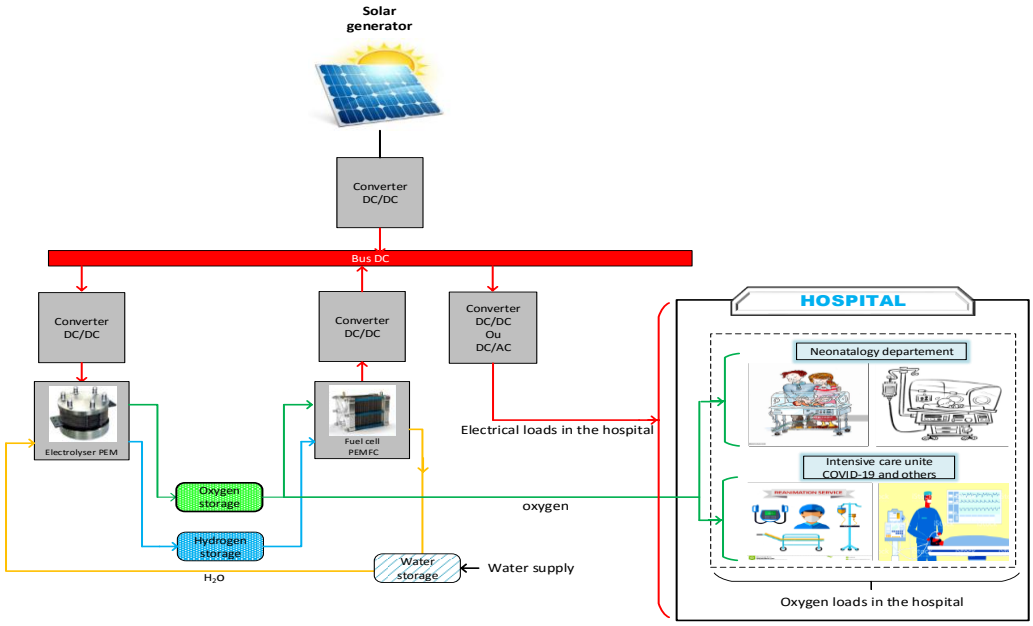

Figure 1: Schematic of a dedicated hospital micro network

1.2. Sizing of system components

The system is sized to allow the electrolyzer to produce 20 m^3 of oxygen per day for medical needs. This could be patients in neonatal units, intensive care units or a COVID-19 patient in respiratory distress.

1.2.1. Determination of the electrolyzer.

Knowing the required amount of oxygen, the amount and characteristic of electrical energy in term of current need for electrolysis operation can be computed using the faraday law. The electrolyzer current is then estimated from the oxygen molar flow rate and the faradic efficiency of the electrolyzer as writed is equation (1).

$$\dot{N}_{O2} = \frac{N_{elec}\, I_{el}\, \eta_F}{N_{stO2} F} \qquad (1)$$

The hydrogen molar flow rate is also calculated on the basis of Faraday's law as given in equation (2).

$$\dot{N}_{H2} = \frac{N_{elec}\, I_{el}\, \eta_F}{N_{stH2} F} \quad (2)$$

The molar flow rate of the water supply to the electrolyzer is calculated from the equation (3):

$$\dot{N}_{H2O} = 2\dot{N}_{O2} = 2 \times \frac{N_{elec}\, I_{el}\, \eta_F}{N_{stO2} F} \quad (3)$$

The electrolyzer power is given in equation (4) knowing the current and the cell voltage (U_{el})

$$P_{Telec} = U_{el} \times N_{elec} \times I_{el} \quad (4)$$

1.2.2. Fuel cell sizing

The fuel cell is sized based on the nominal hydrogen and oxygen flow rate output by the electrolyzer as reporting in equation (5) and (6) respectively.

$$\dot{N}_{H2} = \frac{N_{celP}\, I_{fc}\, \eta_F}{N_{stH2}\, F} \quad (5)$$

$$\dot{N}_{O2} = \frac{N_{elec}\, I_{fc}\, \eta_F}{N_{stO2}\, F} \quad (6)$$

1.2.3. Photovoltaic field sizing

The PV array will be calculated to feed the sized electrolyzer as a priority. The energy excess will be diverted to the hospital electrical appliances. Energy storage will be in chemical form and will be provided by the hydrogen tank placed between the electrolyzer and the fuel cell.

The peak power is expressed as in equation (7):

$$P_{PV} = \frac{P_{EL} \times DF}{E_S \times K_S} \quad (7)$$

2. System components modeling using bond graph

2.1. The Bond graph approach

The bond graph is a modeling technique that allows physical systems (electrical, mechanical, hydraulic, and so on) to be described in a unified language that is well

suited to modeling power transfers because the elements are analogous regardless of the physical domain to which the system belongs [28-30]. The power flow is represented by connectors known as power links that connect the system's constituents. Two conjugate power variables, effort (e) and flux (f), characterize this power exchange (f). Pseudo-linkage graphs [31] are the name for these patterns. The power exchanged between two systems A and B is represented in Figure 2(a) by a bond and a half-arrow indicating the direction of the power flow [30]. The concept of causality is a major structural property of the bond graph. Causation is depicted by a hyphen in the bond graph, indicating the direction of effort. As indicated in the block diagram in Figure 2 (b) [30], system A imposes an effort on B, and B imposes a return flow on A.

Figure 2: Representation of a bond graph (a) and block diagram (b) [32] [33].

Most systems in the bond graph can be represented by a set of elements. R, C, I, TF, GY, SE, SF, De, Df, and J are the elements describes the functions of each of these elements. All sorts of multiphysical dynamic systems may be portrayed using the Bond Graph formalism [29, 34].

The bond graph tool can be used to model in five different ways [35]. These modeling steps are summarized in the flowchart (figure 3).

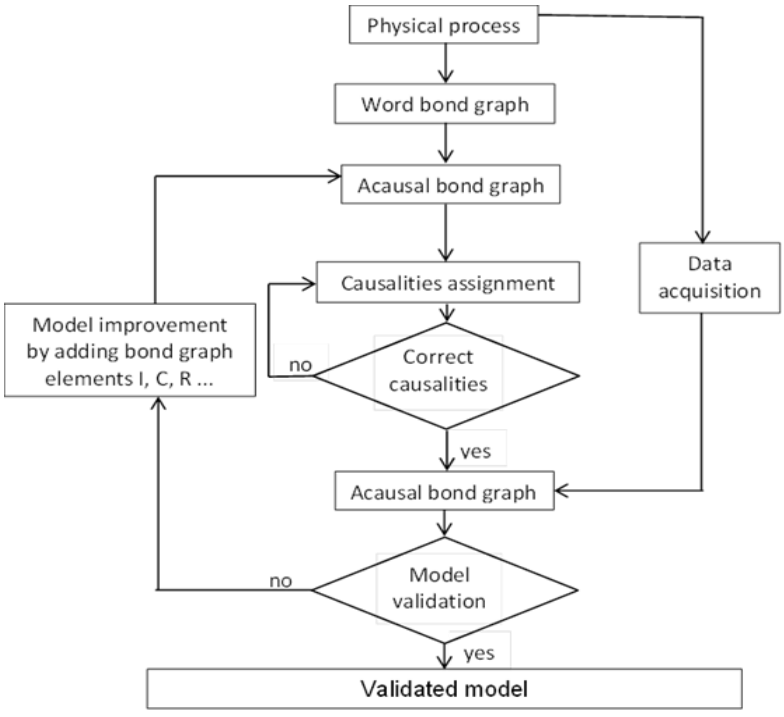

Figure 3: Bond graph modelling steps **[**31**].**

Bond Graph models are built for each element of the proposed hybrid system, including the solar generator, the PEM electrolyzer, and the PEM fuel cell, as shown in Figure 3. Knowing the flow or block diagram of each subsystem, the bond graph formalism allow through the presentation and the description of physicals process, the integration of 4 levels of modeling using an unique graphical formalism. : (i) the Bond Graph's technological level, which consists of breaking subsystems into their numerous components and characterizing the nature of energy exchanges between them; (ii) the physical level, which allows for the representation of physical phenomena using BG elements; (iii) the mathematical level, which allows for the description of system behavior using the constitutive equations of BG elements; and (iv) the algorithmic level, which describes how mathematical models are calculated. [36].

2.2. PV modelling by BG

To simulate PV cells working under diverse situations, several electrical models have been presented in the literature [35, 37-38]. The amount of parameters to be identified determines the model's complexity. Each model is simply an upgrade on the ideal model, which includes a current source and a diode to represent incident solar power. The single-diode model in Figure 4 provides a fair balance of simplicity and accuracy [27, 38-39]. A photocurrent (Iph), a diode, a parallel resistance (Rp) indicating a leakage current, and a series resistance (Rs) due to the contacts between the semiconductors and the metal elements make up the corresponding circuit of the general model**.**

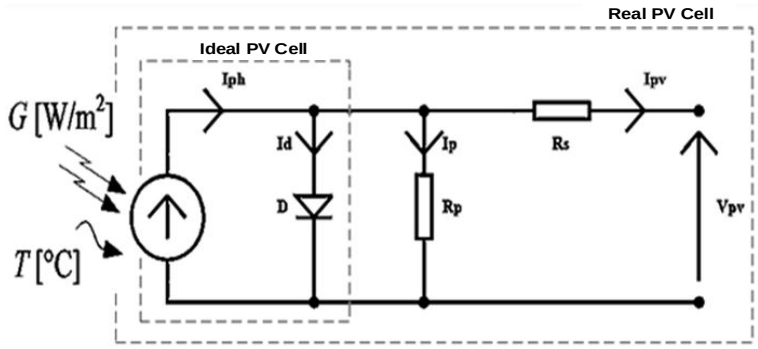

Figure 4: Equivalent electrical circuit of a photovoltaic cell

Based on the electrical circuit, the current generated by the cell can be presented as in equation (8).

$$Ipv = \{I_{sc} + K_i.(T_c - T_{ref})\}.\frac{G}{G_{ref}} - I_0\left\{exp\left(\frac{q(V+IR_s)}{AkT}\right) - 1\right\} - \frac{V+IR_s}{R_p} \quad (8)$$

Implementation in 20-sim of the proposed PV model

The bond graph model of the equivalent electrical circuit of a photovoltaic cell illustrated above (Figure 4) is shown in figure 5.

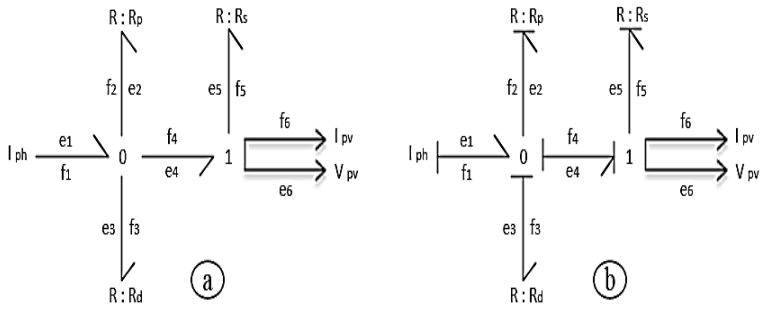

Figure 5: Bond graph model in Figure 4: a) acausal model b) causal model

The implementation in 20-sim requires the addition of some extra blocks to the bond graph.

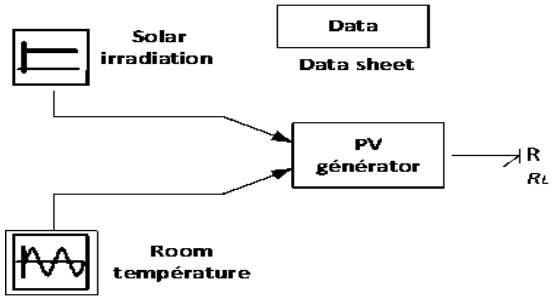

Figure 6: Full implementation of a photovoltaic generator on 20-sim

Radiation G and ambient temperature Ta are inputs of the model depicted in Figure 6. The parameters provided by the manufacturers' data sheets are inserted in the data sheet block. This data is also used as a parameter in the suggested model. The load resistance is denoted by the letter RL. The BG technique is used to extract the parameters in this study. The major goal is to get the best simulation results possible by employing symbols for the entire photovoltaic system.

We will obtain the known literal expression of the current (Ipv) from a photovoltaic cell to a diode by using the rules of bond graph methodology [40] to determine the equations leading to each junction from the "0" and "1" nodes of the causal bond graph presentation of the photovoltaic model in Figure 5.

The resistance of the diode is defined by the expression given by equation:

$$R_d \frac{V_T\, Log\,(\frac{I_d}{I_s}+1)}{I_{ph} - I_p - \frac{V_d}{R_p}} \tag{9}$$

The equations obtained at each node, combined with the element equations are:

- **at the ''0'' node**

$$\begin{cases} e_1 = e_2 = e_3 = e_4 \\ f_1 - f_2 - f_3 - f_4 = 0 \end{cases} \tag{10}$$

$$\begin{cases} e_2 = e_4 \\ f_3 = I_{ph} - \frac{e_2}{R_p} - f_4 \end{cases} \tag{11}$$

- **At node ''1**

$$\begin{cases} f_4 = f_5 = f_6 \\ e_4 = e_5 + e_6 \end{cases} \tag{12}$$

$$\begin{cases} f_4 = f_5 = f_6 \\ e_6 = e_4 - e_5 \end{cases} \tag{13}$$

$$\begin{cases} f_4 = f_6 = I_{pv} \\ e_4 = R_s I_{pv} + V_{pv} \end{cases} \tag{14}$$

From the constitutive law of the elements, e_3 which represents the voltage V_d is given in equation (15)

$$e_3 = V_d = V_T\, Log\,(\frac{f_3}{I_s} + 1) \quad \leftrightarrow \quad e_3 = V_T\, Log\left(\frac{f_1 - f_2 - f_6}{I_s} + 1\right) \tag{15}$$

From the combination of equations (10), (11), (12), (13) and (14) obtained from nodes "0" and "1" and equation (15), the expression of the output voltage of the PV module is write as in equation (16).

$$V_{pv} = V_T\, Log\left(\frac{I_{ph} - \frac{V_{pv}}{R_p} - \frac{R_s I_{pv}}{R_p} - I_{pv}}{I_s} + 1\right) - R_s I_{pv} \tag{16}$$

From equation (16) we can deduce the mathematical expression for the current I_{pv} (f_6) as a function of the voltage of a single diode PV cell, as follows:

$$I_{pv} = I_{ph} - I_s\left\{exp\left[\frac{(V_{pv} + I_{pv} R_s)}{n\, V_T}\right] - 1\right\} - \frac{V_{pv} + I_{pv} R_s}{R_p} \tag{17}$$

2.3. Modeling of the PEM electrolysis system by BOND-GRAPH

The electrolyzer bond graph model developped is this part is based on the previous models proposed by Olivier in [34] and Sumit and al in [32].

- **Principle**

The PEM electrolyzer requires a supply of water at its anode and with a sufficient potential difference applied across its terminals, the water is dissociated to generate oxygen at the anode and hydrogen at the cathode.

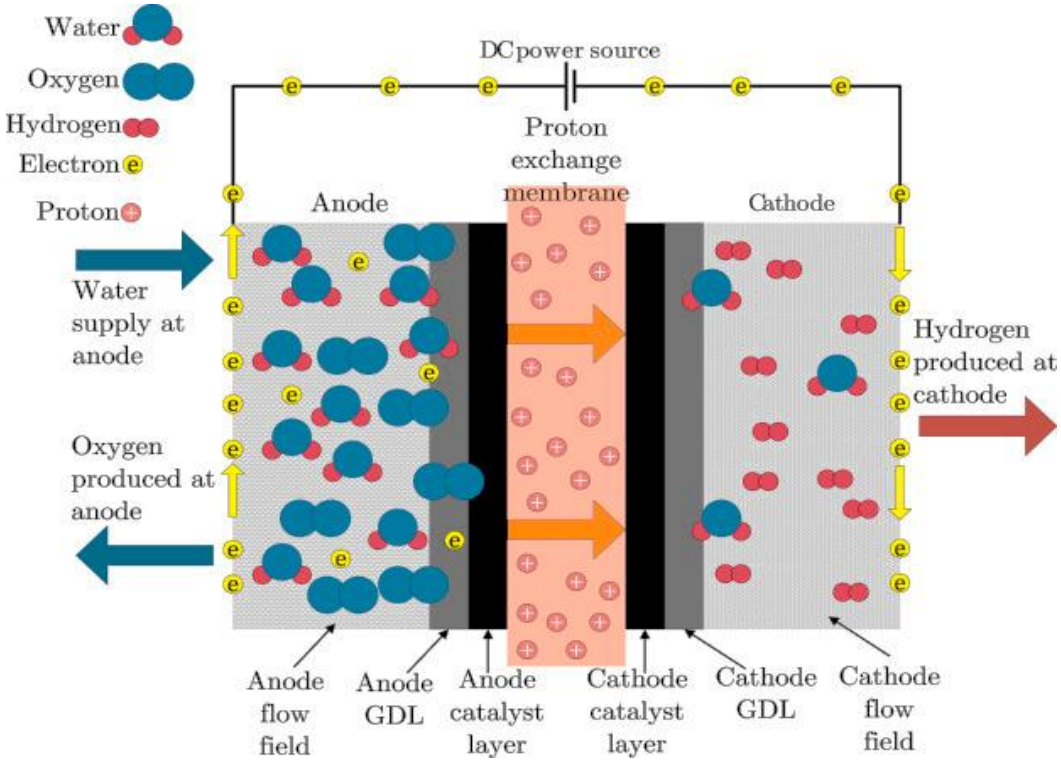

Figure 7: Schematic principle of PEM electrolysis [41**]**

Multi-physical phenomena must exist simultaneously in order for this reaction process to occur. Thermodynamic, chemical, electrochemical, fluidic, thermal, electrical, and substance transfer are examples of these phenomena. These multi-domain interactions are highlighted in the schematic (Figure 8). As a result, we can classify an electrolysis system as a complex system because it involves multiple multiphysical phenomena (Figure 8) as well as a large number of components (Figure 9).

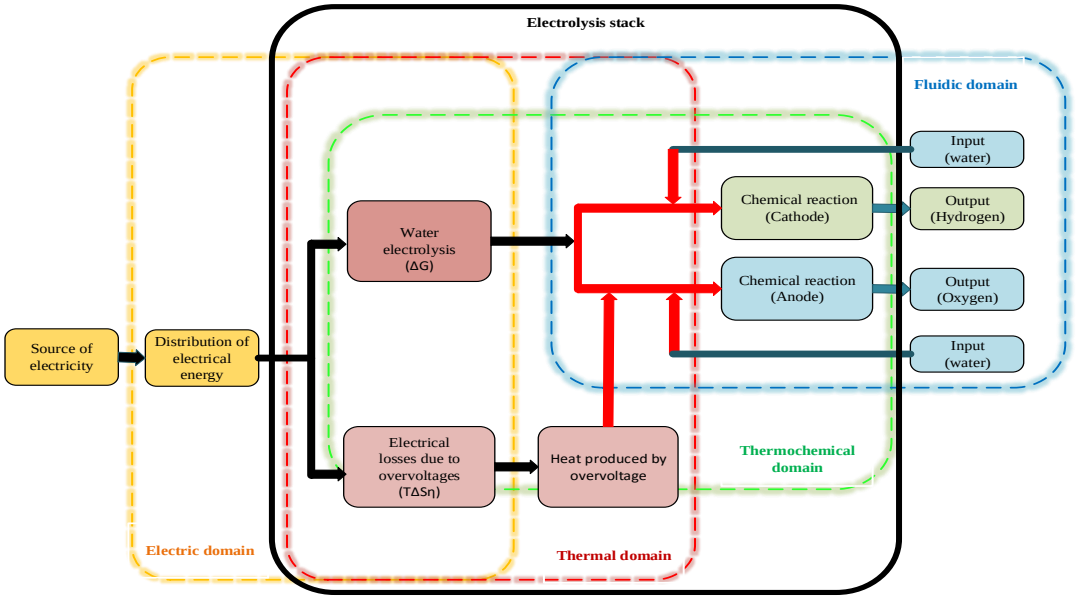

Figure 8: Synoptic of multiphysical interaction phenomena in the electrolysis environment [36]

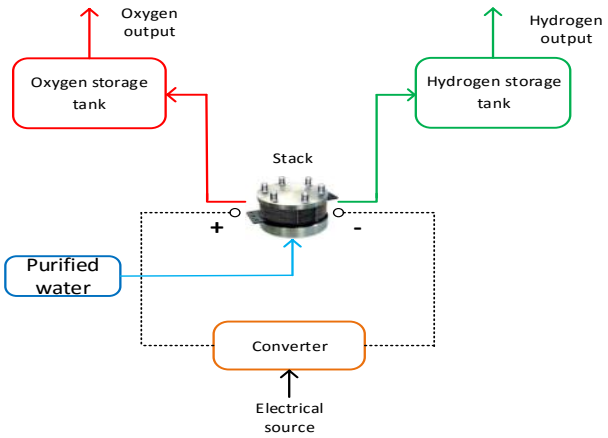

Figure 9: The technology diagram of a PEM electrolysis system used for modelisation

- **Implementation of the proposed electrolyzer model in 20-sim**

The implementation of an electrolyzer in 20-sim requires the addition of some extra blocks to the bond graph.

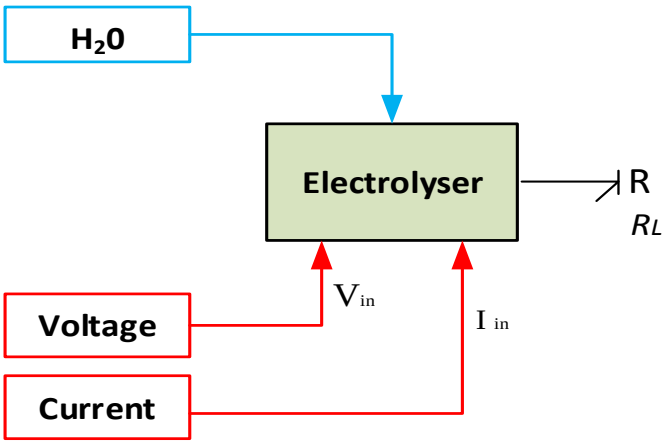

Figure 10: Complete implementation of an electrolyzer in 20-sim

In the model of Figure 10, voltage (Vin), current (Iin) and water (H_20) are the inputs. In the data sheet block, the parameters provided by the manufacturers data sheets are entered. These informations are also considered as input to the proposed model. R_L is the resistance of the load(s).

- **Word Bond Graph of PEM electrolyzer**

Figure 11 illustrates the word bond graph of the predicted PEM electrolysis system. The fluidic exchanges, thermofluidic exchanges, thermofluidic exchanges, and electrical exchanges related to liquid water, hydrogen flow, oxygen flow, and electricity produced by the PV are depicted in this diagram.

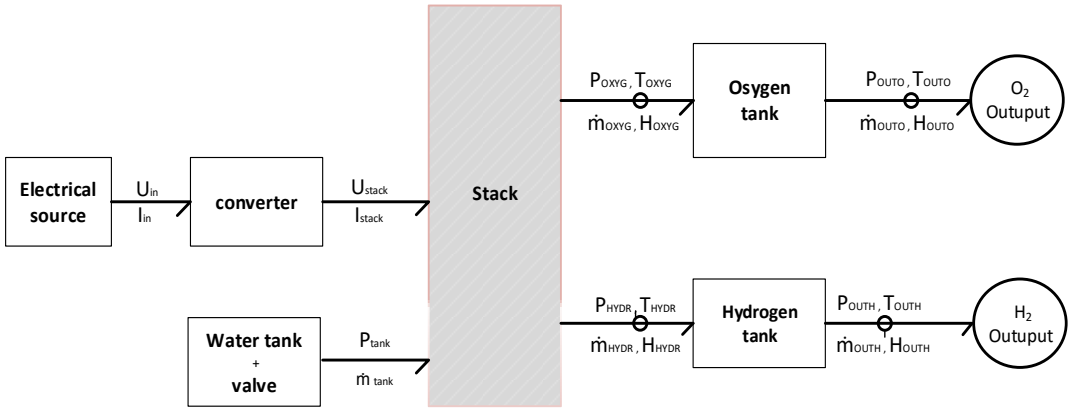

Figure 11: Word Bond Graph of the PEM electrolysis system considered

Bond graph model of the electrolyzer system

– **Electrochemical model**

Within the stack, electrical and electrochemical events are considered instantaneous. As a result, algebraic and non-differential equations are used to describe these events. The electrical behavior of the stack is thus described in the Bond Graph by non-linear entropy generating electrical resistances that represent the various sources of irreversibility, as well as a transformer element that represents the transformation of electrical energy into chemical energy [34, 36]. The expression of the cell voltage of an electrolyzer is given in equation (18) [36, 42-43]:

$$U_{cell} = U_{rev} + U_{ohm} + U_{act} \quad (18)$$

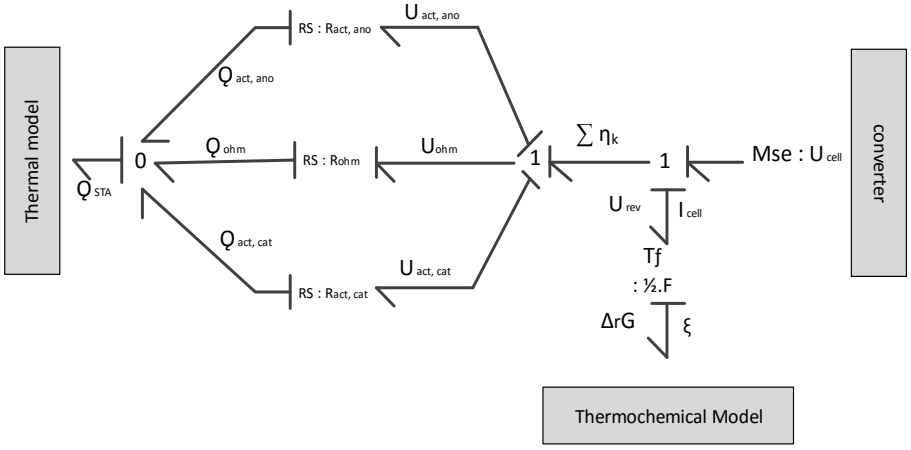

Figure 12: Electrochemical model of a PEM electrolyzer cell in bond graph

The "1" junctions, which are associated with the Bond Graph' model's causality, allow us to derive the following equations:

$$\sum_k \eta_{k=} = U_{cell} - U_{rev} \quad (19)$$

$$U_{ohm} = \sum_k \eta_k - U_{act,\ ano} - U_{act,\ cat} \quad (20)$$

$$U_{ohm} = U_{cell} - U_{rev} - U_{act,\ ano} - U_{act,\ cat} \quad (21)$$

'

At non-zero current, the cell voltage is made up of two terms: the thermochemical model's reversible potential Erev and the numerous overvoltages $\sum_{k=0}^{n} n^k$ generated by irreversible dissipation events associated to current circulation within the cell [34, 36]. [34, 36] describe the primary dissipation mechanisms in a PEM electrolysis cell. Equations (20) and (21) give the mathematical formulations for these mechanisms (21).

– **Fluidic and material transfer model**

Since of their impact on the cell's efficiency and overall behavior, fluidic and material transport events at the core of the cell cannot be overlooked.

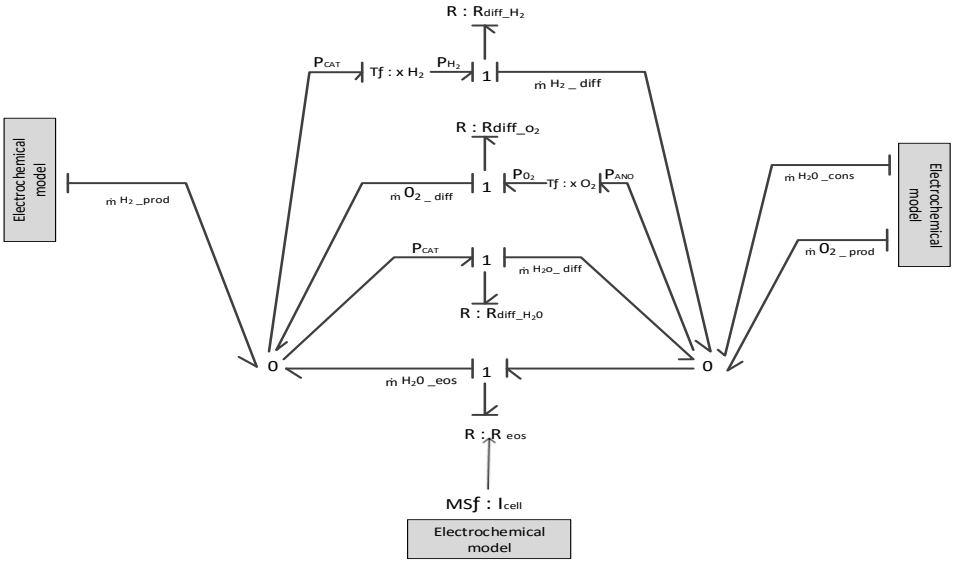

Figure 13: Fluid model of the PEM electrolysis cell in bond graph

The constitutive equation of the 0 junctions allows to deduce the equations

$$\dot{m}_{H2\_prod} = \dot{m}_{H2\_diff} + \dot{m}_{H2O\_diff} - \dot{m}_{O2\_diff} - \dot{m}_{H2O\_eos} \quad (22)$$

$$\dot{m}_{O2\_prod} = \dot{m}_{H2O\_cons} + \dot{m}_{O2\_diff} + \dot{m}_{H2O\_eos} - \dot{m}_{H2\_diff} - \dot{m}_{H2O\_diff} \quad (23)$$

The other models (thermal, thermochemical) have emerged through the same approach.

– **Complete Bond Graph model of the electrolysis stack**

The complete BG model of the stack is shown in Figure 14. Although integrated within the model, the material transfers across the PEM membrane are not shown within this figure for readability reasons.

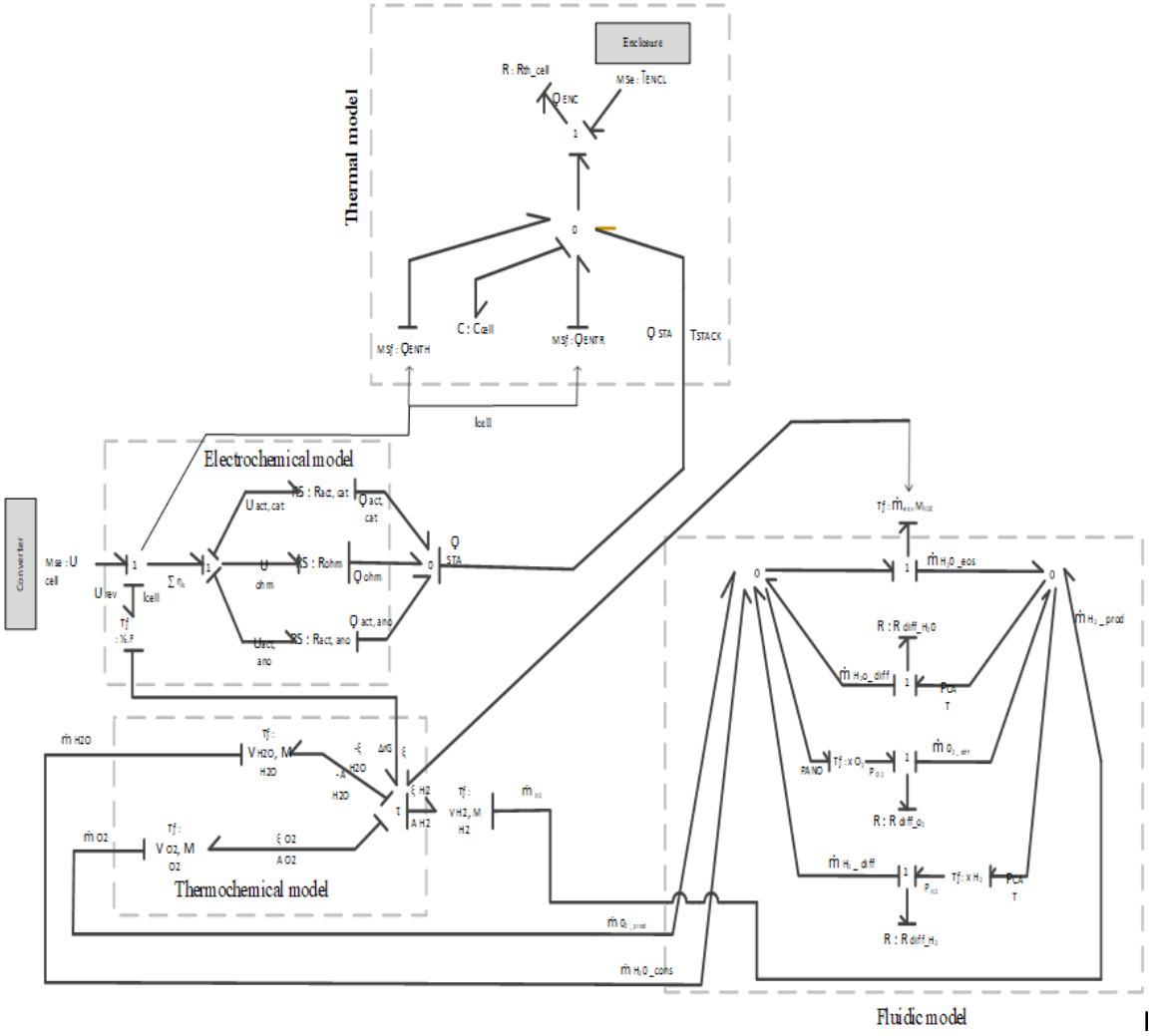

Figure 14: Simplified bond graph model of the PEM electrolysis cell

2.4. Bond graph model of PEM fuel cell

The fuel cell works in the reverse mode of water electrolysis [27]. The word Bond Graph of the cell is developed according to the same principle as that of the electrolyzer and is shown in Figure 15.

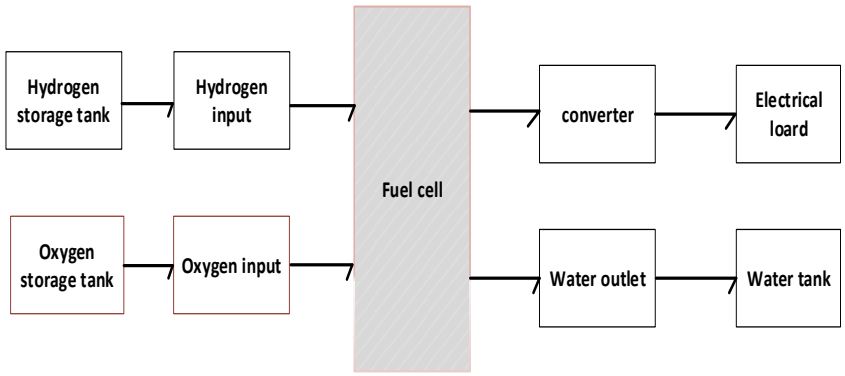

Figure 15: Word Bond Graph of the considered PEM fuel cell

The cell's graphical bond is developed from that of the electrolyzer by reversing the direction of fluid flow and subtracting the voltage surges from the reversible voltage.

3. Simulations and results

3.1. Meteorological datas and component characteristics

3.1.1. Meteorologique datas

The hourly evolution of temperature and solar radiation during the sunniest day and the least sunny day are depicted in Figure 16 and 17.

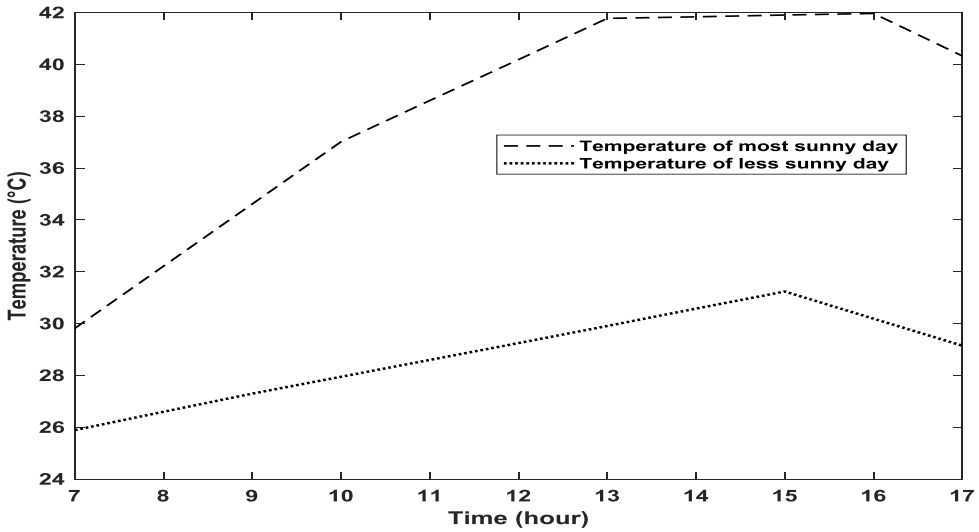

Figure 16 : Daily temperature curve

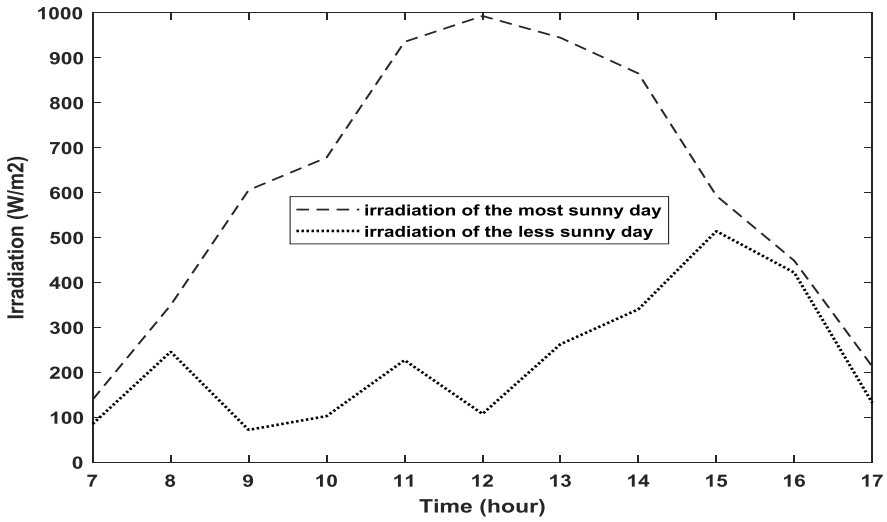

Figure 17: Daily sunshine curve

As shown in Figure 17, during the least sunny day of the year, the level of irradiation is unstable between 7 a.m. and 12 p.m., but in general the irradiation is interesting in the afternoon, precisely between 13 p.m. and 16 p.m. with a maximum value of 514.27 W/m^2 and a minimum value of 72.12 W/m^2. But for the sunniest day of the year, the irradiation varies normally and this variation is such that: between 7 am and 12 pm, we observe an increase which varies from 139.58 W/m^2 to 993.11 W/m^2; at 12 pm, we observe the maximum point, which is 993.11 W/m^2; and between 12 pm and 17 pm, we note a decrease which varies from 993.11 W/m^2 to 213.05 W/m^2. Note also that between 9 a.m. and 15 p.m., the irradiation value recorded is greater than 500 W/m^2.

3.1.2. Component characteristics

The characteristics of the electrolyzer, the fuel cell and the PV field are summarized in table 1.

Table 1: Summary table of system component characteristics

PV generator	Power (W)	40445
	Voltage (V)	24
	Courrent (A)	58
	Number of cells in series	3
	Number of cells in parallel	52
	Total number of panels	154
Electrolyzer	Power (W)	19338
	Voltage (V)	72
	Courrent (A)	58
	Number of cells in series	45

Fuel cell	Power (W)	15.000
	Voltage (V)	220
	Courrent (A)	24
	Number of cells in series	45

The assumption made are the follows:

- Number of electrolysis cells in series: Ncel=45
- Electrolyzer cell voltage is: Ucel= 1.6 V
- The loss coefficient is: K_S =0.8
- The number of hours of daily operation of the electrolyzer is: DF=08 hours

3.2. Simulation of PV system

3.2.1. PV panel I-V and P-V characteristic curves

The characteristics of the PV panels used for simulation are specified in the table 2.

Table 2: Characteristics of the C-SUN 260 PV panel used

Maximum power (P_{max}) W	260
Voltage at Pmax (V_{mp}) V	30.8
Current at Pmax (I_{mp}) A	8.44
Guaranteed minimum P_{max}	NA
Short-circuit current (I_{sc}) A	8.9
Open-circuit voltage (V_{oc}) V	38.1
Temperature coefficient of open-circuit voltage %/K	-0.307
Temperature coefficient of short-circuit current %/K	0.039
Temperature coefficient of power %/K	-0.432
NOCT °C	47
Number of cells	60
Dimension mm×mm	1640×990

The simulations of the current-voltage and power-voltage characteristics is carried out under real tropical atmosphere for a typical sunny day. For this purpose, the hourly data of temperature and irradiance are recorded and used as input vector. The I-V and P-V characteristic curves obtained from the simulation of the bond graph model of the photovoltaic panel described by the single diode model are depicted in figure 18 and

figure 19 respectively. The characteristic curves are sensitive to meteorological parameters including temperature and solar radiation. In fact, an increase in temperature induces a reduction in the transition band of the semiconductors, thus affecting the majority of the PV panel parameters.

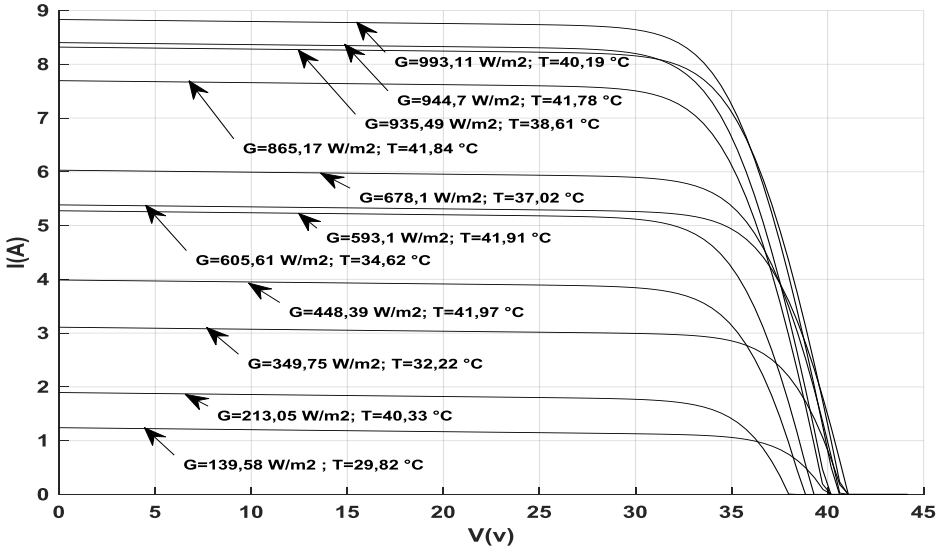

Figure 18: Evolution of the panels I-V characteristics under real meteorological excitations

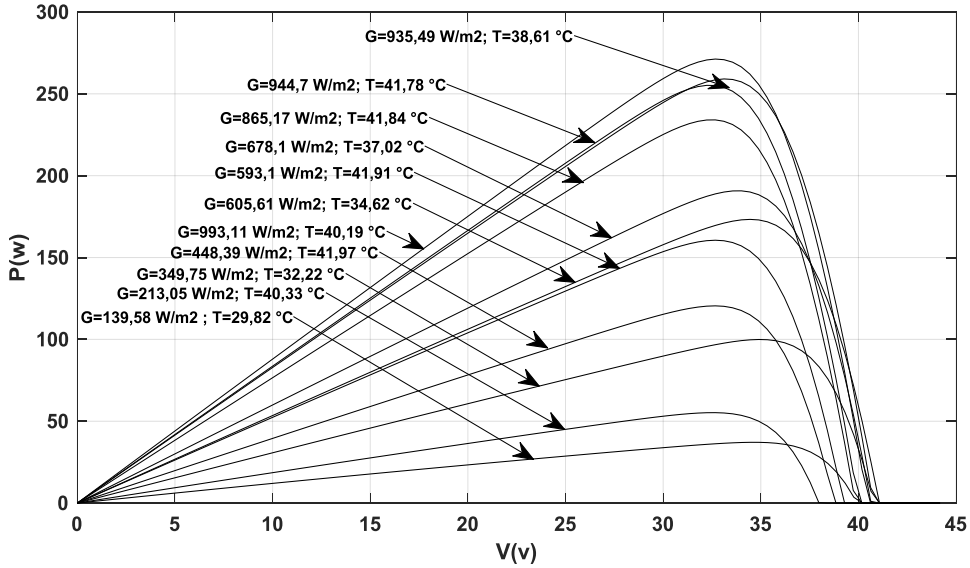

Figure 19: Evolution of the P-V characteristics of the panel under real weather excitations

3.2.2. Power output by the PV farm

In this part, the maximum power output by the PV subsystem are extracted and represented in figure 20 and figure 21 respectively for the least sunny day and the sunniest day of the year. As shown in Figure 20, during the less sunny day of the year, due to the intermittency of solar radiation, the power output by the PV subsystem is irregular between 7 a.m. and 12 p.m. An interesting power production are observed between 13 p.m. and 16 p.m. The maximum value of $2.20x10^4$ W and a minimum value of $0.26x10^4$ W are recorded. The irregular profile of PV power will increase the number of electrolyzer start/stop cycles with some consequences on the system reliability. The fuel cell used as backup subsystem will also be affected by the irregular power production and it will shorten maintenance cost.

During the sunniest day of the year**,** the production follows the classical daily solar radiation profile. The power output ranging from $0.58x10^4$ W the minimal value to $4.23x10^4$ W the maximum value observed around midday. The system reliability is ameliorated through the reduction of start/stop cycle.

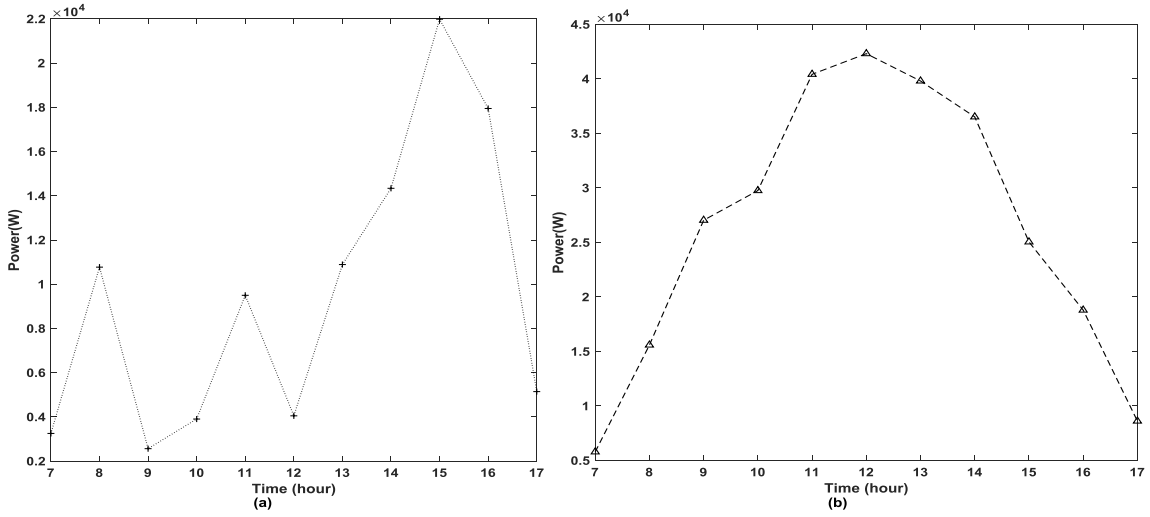

Figure 20: (a): PV Power in the less sunny day (b): PV Power in the sunniest day

3.3. Simulation of electrolyzer

3.3.1. Polarisation curve of the electrolyzer

The performance of an electrolyzer is assessed by the polarisation curves or current-voltage characteristics, which are obtained by measuring the voltage during a current sweep. An electrolyzer will be considered more reactive than another if, at a given voltage, its current density is greater.

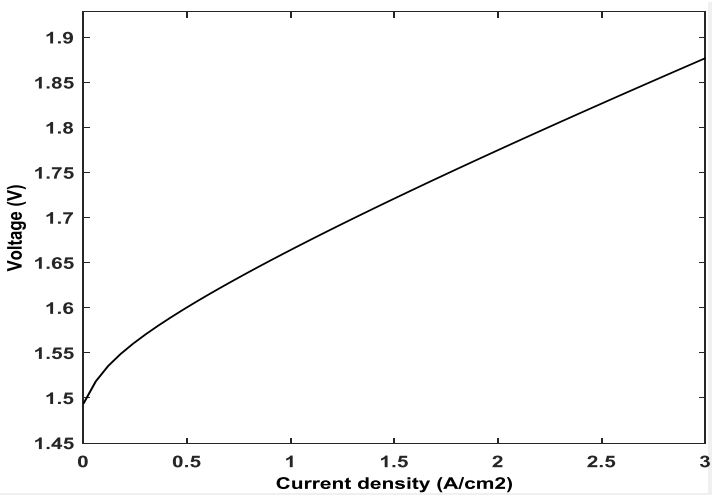

Figure 21: Current-voltage characteristic.

3.3.2. Evolution of oxygen and hydrogen production

The simulation of the bond graph model of electrolyzer powered by PV electricity have also permit to obtained the evolution of oxygen flow rate during the sunniest and the least sunny day. As depicted in Figure 22 and Figure 23, the oxygen and hydrogen production follow the curve of power production. In Figure 22, it is observed that during the least sunny day of the year, the oxygen is generated intermittently due to the fact that solar production is variable, so not continuous. The oxygen production flow rate range between a maximum value of 0.84 Nm^3/h and a minimum value of 5.98 Nm^3/h. Fortunately, the electrolyzer output can be dispatched quickly to match change in solar electricity production. However, during the sunniest day of the year, the oxygen production is very interesting due to favorable solar radiation despite the increase of temperature. With these conditions, a peak value of 11.59 Nm^3/h is recorded around the midday. The shape of the oxygen production curve is similar to that of irradiation and PV output. The same assessment is made for hydrogen production for which a correlation with the solar radiation is highlight in Figure 23. In summary, the electricity, oxygen and hydrogen production are all subject to the existence of favorable irradiation and temperature conditions. The daily amount of oxygen produced is closed to 14.61 Nm^3 and 39.37 Nm^3 during the least sunny day and the sunniest day respectively. The amount of hydrogen (considered as by-product) output by the electrolyzer per day is around 29.23 Nm^3 in a less sunny condition and 78.74 Nm^3 in a sunny condition. By using either of these values combined to the value of the net calorific value of hydrogen, it appears that the fuel cell can provide backup power during power outages under the influence of low solar radiation.

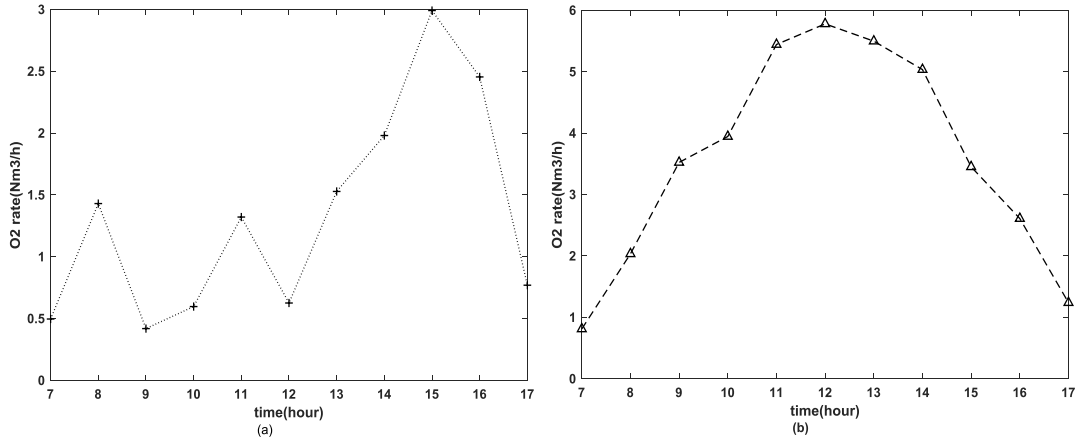

Figure 22: (a): Oxygen rate in the least sunny day (b): Oxygen rate in the sunniest day

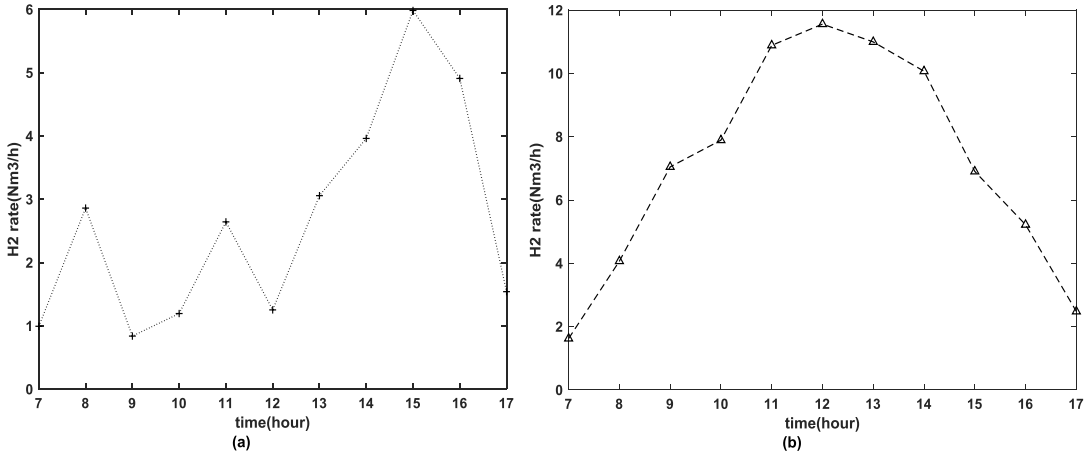

Figure 23: (a): Hydrogen rate in the least sunny day (b): Hydrogen rate in the sunniest day

Finally, we used the BG tool to simulate the components of our hybrid system. The results indicate that this approach can be used to model hybrid systems made up of elements such as the electrolyzer and fuel cell for application in hospital-type structures.

Conclusion

The objective of the work was to use the BG approach to model a hybrid system consisting of a PV generator, a PEM electrolyzer and a PEM fuel cell dedicated to the production of electricity and oxygen for a hospital. The simulation of these models under tropical atmospheric condition was conducted for two extremal cases; the sunniest days and the least sunny days of the year. The simulation of the bond graph model of PV module developed from the single diode model was first performed and have achieved current-voltage and power-voltage characteristics of PV subsystem. The PV maximum power diverted to the electrolyzer was extracted from electrical

characteristic curves obtained using the BG approach. In addition, the simulation of the bond graph model of electrolyzer made it possible to obtain the polarization curve representing the current-voltage characteristics. The same simulation has also achieved the oxygen and hydrogen flow rate for the sunniest and the least sunny day of the year. By analyzing the results, the design and modeled hybrid system are capable to produce in sunny conditions 39.37 Nm^3 of oxygen and 78.74 Nm^3 per day. Under unfavorable conditions, the system despite the insufficient solar radiation, the daily amount of oxygen and hydrogen produced is respectively closed to 14.61 Nm^3 and 29.23 Nm^3. These results serve as proof that the modeled system is capable even is less sunny conditions, to ensure the availability of oxygen for medical care and hydrogen as electricity storage vector. The bond graph can then be used for modeling an onsite oxygen production system consisting of PV modules, PEM electrolyzer and PEM fuel cell which serve as backup subsystem.

Nomenclature

A Ideal factor depending on the PV technology

F Faraday constant: 96487 C/ mole

G Aunshine

G Solar radiation in watt/square meter (W/m^2)

Gref Reference insolation of the cell (= 1000W / m^2)

I_0 diode current which is proportional to the saturation current

I_d Current through the diode

I_{elec} Electrolyzer current

Iph Current generated by light or photo current

I_{pile} Battery current

I_{pv} Current of a photovoltaic cell

Isc Short-circuit current of the cell at 25 °C and 1000W / m^2

k Boltzmann's constant (1.38×10^{-23} J / K)

Ki Temperature coefficient of the short-circuit current of the cell

$\dot{m}_{i\_diff}$ Diffusion flux of species i through the proton exchange membrane

$\dot{m}_{i\_prod}$ Hydrogen and oxygen production flow

$\dot{m}_{H2O\_cons}$ Water flow rate consumed by the reaction

$\dot{m}_{H2O\_eos}$ Electroosmosis flow.

N_{celec} Number of cells in the electrolyzer in series

N_{celP} Number of cells in the battery

$\dot{N}_{O2}$ Volume of oxygen

$\dot{N}_{H2}$ Hydrogen flow rate produced

$\dot{N}_{H2O}$ Molar flow rate of the water to be fed to the electrolyzer

N_{stH2} Stoichiometry coefficient for hydrogen

N_{stO2} Oxygen stoichiometry coefficient

P Pressure

Pb Tank pressure which is measured in (Pascal)

Pbi Initial pressure of the storage tank in (Pascal)

P_{Telec} Power of the electrolyzer

q Electron charge (1.6×10^{-19} C)

R Universal gas constant (J/mol.K)

Rs Series resistance (Ω)

RL The load resistance.

Rp Parallel resistance

Vb Volume of the tank (m^3)

V_d Voltage at diode terminal

Vm Molar volume

Ta Ambient temperature

Tb Operating temperature (K)

Tc Cell temperature in Kelvin (K)

Tref Reference temperature of the cell

Z Compressibility factor as a function of pressure,

ηF Faradic efficiency: 0.9

Abbreviation

BG Bond graph

EL Electrolyzer

PEM. Proton exchange membrane

PV Photovoltaic

REFERENCES

[1] Wang, C., Nehrir, N. M., Steven, R. 2005. Dynamic Models and Model Validation for PEM Fuel Cells Using Electrical Circuits. *IEEE Transactions on Energy Conversion*, Vol. 20, N°. 2. https://ieeexplore.ieee.org/abstract/document/1432859/

[2] Agbli, K. S., Péra, M. C., Hissel, D., Rallières, O., Turpin, Doumbia, I. 2011. Multiphysics simulation of a PEM electrolyser: Energetic Macroscopic Representation approach. *International journal of hydrogen energy. 36: 1382 - 1398*. https://doi.org/10.1016/j.ijhydene.2010.10.069

[3] Daniel, H., and al. 2008. A review on existing modeling methodologies for PEM fuel cell systems. In: Fundamentals and developments of fuel cells cenference.

[4] ReuB, M., Reul, J., Grube, T., and al. 2019. Solar hydrogen production: a bottom-up analysis of different photovoltaic-electrolysis pathways. Sustainable Energy Fuels 3:801-813.https://doi.org/10.1039/c9se00007k.

[5] Loong, Y. T., Dahari, M., Yap, H. J., Chong, H. Y. 2013. Modeling and simulation of solar powered hydrogen system. Appl Mech Mater 315:128-135. https://doi.org/10.4028/www.scientific.net/AMM.315.128.

[6] Touili, S., Alami Merrouni, A., Azouzoute, A., El Hassouani, Y., Amrani, A-I. 2018. A technical and economical assessment of hydrogen production potential from solar energy in Morocco. *Int J Hydrogen Energy* 43:22777-22796. https://doi.org/10.1016/j.ijhydene.2018.10.136.

[7] Grimm, A., Jong, W. A., Kramer, G. J. 2020. Renewable hydrogen production: a techno-economic comparison of photoelectrochemical cells and photovoltaic-electrolysis. *Int J Hydrogen Energy* 45: 22545-22555. https://doi.org/10.1016/j.ijhydene.2020.06.092.

[8] Yang, Z., Lin, J., Zhang, H., Lin, B., and Lin, G. 2018. A new direct coupling method for photovoltaic module-PEM electrolyzer stack for hydrogen production. Fuel Cells 18:543-550. https://doi.org/10.1002/fuce.201700206.

[9] Fopah-Lele, A., Kabore-Kere, A., Tamba, J. G., Yaya-Nadjo, I. 2021. Solar electricity storage through green hydrogen production: A case study. *Int J Energy Research*. p. 1-15. https://doi.org/10.1002/er.6630

[10] Zorica, S., Vuksic, M., Zulim, I., Marko Vuksic, A. 2014. Evaluation of DC-DC resonant converters for solar hydrogen production based on load current characteristics design considerations of the multi resonant converter as constant current source for electrolyzer utilization view project solar climber: a problem.

[11] Nouhaila, L., Mahmoud, B., Morad, H., Jalal, S., Hamid, G. 2021. Modeling and control of a hydrogen-based green data center. *Electric Power Systems Research* 199 107374 https://doi.org/10.1016/j.epsr.2021.107374

[12] Garrigós, A., Lizán, J. L., Blanes, J. M., Gutiérrez, R. 2014. Combined maximum power point tracking and output current control for a photovoltaic-electrolyzer DC/DC converter. *Int. J. Hydrogen Energy* 39, 20907–20919.

[13] Karami, N., Moubayed, N., Outbib, R. 2014. Energy management for a PEMFC-PV hybrid system. *Energy Convers Manag* 82:154-68. https://doi.org/10.1016/J.ENCONMAN.2014.02.070

[14] Ceren, C., Yılser, D. 2021. Design and simulation of the PV/PEM fuel cell based

hybrid energy system using MATLAB/ Simulink for greenhouse application. *International journal of hydrogen energy* 46, 22092-22106.

[15] Ismail, T. M., Ramzy, K., Elnaghi, B. E., Abelwhab, M. N., El- Salam, M. 2019. Using MATLAB to model and simulate a photovoltaic system to produce hydrogen. *Energy Convers Manage* 185:101-129. https://doi.org/10.1016/j.enconman.2019.01.108.

[16] Busquet, S. 2003. *Study of an autonomous energy production system coupling a photovoltaic field, an electrolyzer and a fuel cell: realization of a test bench and modeling*. Doctoral thesis, Ecole des Mines de Paris.

[17] Labbé, J. 2006. *Electrolytic hydrogen as a means of electricity storage for isolated photovoltaic systems*. Doctoral thesis from the Ecole des Mines de Paris, 226p.

[18] Darras, C. 2010. *Modelling of Photovoltaic - Hydrogen hybrid systems: Isolated site, microgrid, and grid connection applications in the framework of the PEPITE project (ANR PAN-H).* PhD thesis of the University of Corsica, 252p.

[19] Boya Bi, B. E., Gbaha, P., Ekoun Koffi, M. P., Koua, K. B. 2018. Modelling of the Components of a Hybrid System Photovoltaic Panels - Energy Storage via Hydrogen - Batteries. *European Scientific Journal* January Vol.14, No.3 ISSN: 1857 - 7881 (Print) e - ISSN 1857- 7431

[20] DJAFOUR, A., AIDA, M. S., and AZOUI, B. 2015. Study of a photovoltaic system for energy production based on green hydrogen. *Annals of Science and Technology* Vol. 7, No. 2

[21] Andouisi, R., and al. 2020. Bond graph modelling and dynamic study of a photovoltaic system using MPPT buck-boost converter. In: *IEEE International Conference on Systems,* Man and Cybernetics 3: 6.

[22] Saida, M., Aissa, K. 2017. Bond graph-based modeling for parameter identification of photovoltaic module, *Energy* 141: 1456-1465

[23] Dhafer, M., Hichem, O., Abdelkader, M. 2018. Bond graph modeling and robust control of a photovoltaic generator that powered an induction motor pump via SEPIC converter.

[24] Mohamed, L., Ahmed, K., Amechnoue, K., Mussutac, M., Herbazia, R. 2019. Bond graph modelling of different equivalent models of photovoltaic cell. Procedia Manufact.

[25] Nizar, C., Belkacem, O. B., Anne-Lise, G., Rochdi, M. 2013. Signed Bond Graph for health monitoring of PEM fuel cell.

[26] Fontès, G. 2005. Modeling and characterization of the PEM stack for the study of interactions with static converters.

[27] Abd, E. B., Farid, M., Belkacem Ould, B., Saad, M. 2021. Bond graph modeling, design and experimental validation of a photovoltaic/fuel cell / electrolyzer / battery hybrid power system. *International journal of hydrogen energy* 46(47) : 24011-24027

[28] KOUITINI, H., RECHAM, A. 2016. *bond graph approach for the modelling and simulation of a photovoltaic power plant installed in Algeria*. master thesis presented at the University of Bouira, submitted

[29] Ould Bouamama, B., Abdalah, I., Gehin, A. L. 2018. Bond graphs as

mechatronic approach for supervision design of multisource renewable energy system. In IOP *Conference Series: Materials Science and Engineering* 417(1): p. 012033

[30] Sood, S., Ould-Bouamama, B., Dieulot, J. Y., Bressel, M., Li, X., Ullah, H., Loh, A. 2020. Bond graph base multiphysic modelling of anion exchange membrane water electrolysis. *28th Mediterranean Conference on Control and Automation (MED)* p. 15-18.

[31] Olivier, P., Bourasseau, P., Ould Bouamama, B. 2017. Dynamic and multiphysic pem electrolysis system modelling: A bond graph approach. *International Journal of Hydrogen Energy* 42(22): 14872- 14904.

[32] Sumit, Sood., Belkacem, Ould-Bouamama., Jean-Yves, Dieulot., Mathieu, Bressel., Xiaohong, Li., Habih, Ullah., and Adeline, Loh. 2020. Bond graph base multiphysic modelling of anion exchange membrane water electrolysis. 28th Mediterranean *Conference on Control and Automation* (MED) 15-18, France

[33] Ould Bouamama, B., Abdalah, I., and Gehin, A.-L. 2018. Bond graphs as mechatronic approach for supervision design of multisource renewable energy system. in *IOP Conference Series: Materials Science and Engineering*, vol. 417, no. 1. IOP Publishing, p. 012033

[34] Olivier P. 2017. Modelling and analysis of the dynamic behaviour of a PEM electrolysis system subjected to intermittent loads: bond graph approach.

[35] Madiab, S., Kheldouna, A. 2017. Bond graph based modeling for parameter identification of photovoltaic module. *Energy* 141(15):1456-65.

[36] Sood, S., Prakash, O., Boukerdja, M., Dieulot, J. Y., Ould-Bouamama, B., Bressel, M., Gehin, A. L. 2020. Generic Dynamical Model of PEM Electrolyzer under Intermittent Sources. *Energies* 13, 6556.

[37] Villa-Villasenor, N., Galindo-Orozco, R. 2018. Bond graph modeling of a 4-parameter photovoltaic array. Mathemat Comp Model Dynam Sys Method Tool Appl Eng Relat Sci 24(3).

[38] KBIDI, F. 2019. *Development and testing of microgrid scale energy management strategies with hydrogen storage and production*. Thesis defended at the University of La Réunion.

[39] Allani, M. Y., Tadeo, F., Mezghanni, D., Mami, A. 2019. Application of systemmodeling and simulation of the photovoltaic production, *IJCSNS International Journal of Computer Science and Network* 19(5).

[40] Borutzky, W. 2010. Bond Graph Methodology. *London: Springer London*.

[41] Selamet OF, Becerikli F, Mat MD, Kaplan Y. 2011 Development and testing of a highly efficient proton exchange membrane (PEM) electrolyzer stack. *Int J Hydrogen Energy* 36:11480 -7**.**

[42] ABDALLAH, I. 2018. *Event-Driven Hybrid Bond Graph Application: Hybrid Renewable Energy System for Hydrogen Production and Storage*. PhD Thesis. University of Lille.

[43] Fragiacomo, P., Genovese, M. 2019. Modeling and energy demand analysis of a scalable green hydrogen production system. *Int. J. Hydrogen Energy*. 44:30237-30255 doi:10.1016/j.ijhydene.09.186.